HOKKAIDO UNIVERSITY

Title	Study of the System CaMgSi2O6-CaFe^[3+]AlSiO6-CaAl2SiO6-CaTiAl2O6 : III. The Join CaMgSi2O6-CaFe^[3+]AlSiO6-CaTiAl2O6 at 1 atm
Author(s)	Akasaka, Masahide; Onuma, Kosuke
Citation	北海道大学理学部紀要, 18(3), 409-432
Issue Date	1978-03
Doc URL	http://hdl.handle.net/2115/36663
Type	bulletin (article)
File Information	18_3_p409-432.pdf

Instructions for use

Hokkaido University Collection of Scholarly and Academic Papers : HUSCAP

Jour. Fac. Sci., Hokkaido Univ., Ser. Iv,
vol. 18, no. 3, Mar., 1978, pp. 409-432.

STUDY OF THE SYSTEM $CaMgSi_2O_6$-$CaFe^{3+}AlSiO_6$-$CaAl_2SiO_6$-$CaTiAl_2O_6$: III. THE JOIN $CaMgSi_2O_6$-$CaFe^{3+}AlSiO_6$-$CaTiAl_2O_6$ AT 1 ATM

by

Masahide Akasaka and Kosuke Onuma

(with 3 tables and 10 text-figures)

(Contribution from the Department of Geology and Mineralogy,
Faculty of Science, Hokkaido University, No. 1545)

Abstract

The join $CaMgSi_2O_6$-$CaFe^{3+}AlSiO_6$-$CaTiAl_2O_6$ was studied in air at 1 atm by the ordinary quenching method. Clinopyroxene(ss), forsterite, perovskite, magnetite(ss), spinel(ss), anorthite, melilite, unknown phase X and hibonite were encountered. Phase X was analysed by EPMA. At liquidus temperatures the following assemblages are confirmed: clinopyroxene(ss) + forsterite + spinel(ss) + liquid, clinopyroxene(ss) + magnetite(ss) + spinel(ss) + liquid, forsterite + perovskite + spinel(ss) + liquid, and magnetite(ss) + spinel(ss) + phase X + liquid. At subsolidus temperatures clinopyroxene(ss) single phase field extends up to 18 wt.% $CaTiAl_2O_6$, showing that the content of TiO_2 in clinopyroxene(ss) increases with increasing $CaFe^{3+}AlSiO_6$. Following phase assemblages were confirmed in the subsolidus regions: clinopyroxene(ss) + perovskite, clinopyroxene(ss) + perovskite + spinel(ss), clinopyroxene(ss) + perovskite + melilite (+ anorthite), clinopyroxene(ss) + perovskite + spinel(ss) + melilite + anorthite, clinopyroxene(ss) + perovskite + anorthite + spinel(ss), and clinopyroxene(ss) + perovskite + hibonite + anorthite. Even in the field of clinopyroxene(ss) + perovskite, TiO_2 content in clinopyroxene(ss) continues to increase and attains up to 9.20% TiO_2 and 18.57% Al_2O_3. An implication of the join to Ti-rich fassaitic pyroxene from the alkalic rocks is discussed.

Introduction

Main constituent molecules of clinopyroxene in undersaturated alkalic rocks are $CaMgSi_2O_6$ (Di), $CaTiAl_2O_6$ (Tp), $CaAl_2SiO_6$ (CaTs) and $CaFe^{3+}AlSiO_6$ (FATs) (Onuma and Yagi, 1971, 1975). The system Di-CaTs-FATs-Tp, therefore, is important to understand the role of the pyroxene in the differentiation of alkalic rocks. Among the joins in this system, the join Di-Tp-FATs is most significant, because the clinopyroxenes crystallized in this join contain considerable amount of both Ti and Fe^{3+} which are indispensable in the clinopyroxene from alkalic rocks.

Yagi and Onuma (1967) studied the join Di-Tp and showed that diopside incorpolates Tp as much as 3.7%. Hijikata and Onuma (1969) found that there is a complete solid solution between Di and FATs below 1250°C. According to Onuma and Yagi (1975), CaTs in diopside increases with increasing FATs. In

the present paper, the data of the join Di-FATs-Tp are presented and clinopyroxenes in the join are discussed with special reference to its bearing on the natural Ti-rich fassaitic pyroxenes.

Experimental Methods

In the present investigation the ordinary quenching method was employed at 1 atm in air. The starting materials were prepared by complete crystallization of homogeneous glasses at 900°C. Some starting materials were further heated to 1150°C to promote crystallization and to get better crystals for EPMA analyses. The furnaces used in quenching experiments were regulated to a precision of ±1°C. Pt-$Pt_{87}Rh_{13}$ thermocouples were calibrated at the standard melting points of NaCl (800.4°C), Au (1062.6°C) and diopside (1391.5°C) (The Geophysical Lab. temperature scale).

A JEOL JXA-50A electron microprobe at School of Enjineering, Hokkaido University was operated at 15 KV with bean current of 0.03 – 0.04μ and bean diameter of 1μ. A natural kaersutite was used as a standard for Ca, Mg, Fe, Ti, Al, and Si. Data were corrected by the method of Bence and Albee (1968).

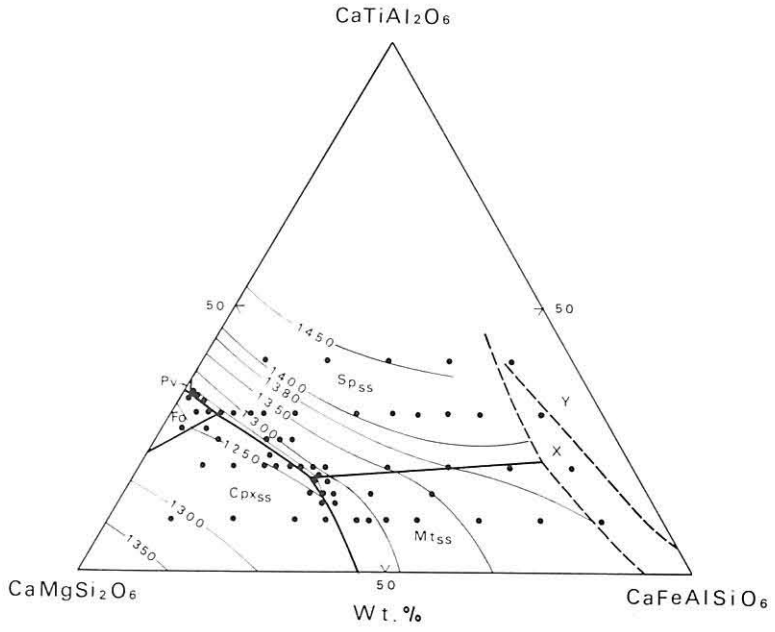

Fig. 1 Liquidus diagram of the join $CaMgSi_2O_6$-$CaFe^{3+}AlSiO_6$-$CaTiAl_2O_6$. Abbrevations are the same as in Appendix, except Y (hibonite).

Experimental Results and Discussion

Liquidus Diagram

The results of quenching experiments are given in appendix. A liquidus diagram is shown in Fig. 1. Clinopyroxene(ss), forsterite, perovskite, magnetite(ss), and spinel(ss) are present at liquidus temperatures (ss: solid solution). Besides these phases, two unknown phases were encountered as primary phases. One was found by Hijikata and Onuma (1969) in the join Di-FATs and named "phase X" and the other, "phase Y",* was found in the join FATs-Tp by Onuma and Yagi (1971). In the liquidus diagram there are four points showing four-phase assemblage:

(1) clinopyroxene(ss) + forsterite + spinel(ss) + liquid at 1235° ± 5°C and Di(63)FATs(7.5)Tp(29.5)

(2) clinopyroxene(ss) + magnetite(ss) + spinel(ss) + liquid at 1245° ± 5°C and Di(54)FATs(29)Tp(17)

(3) forsterite + perovskite + spinel(ss) + liquid at 1238° ± 5°C and Di(66)FATs(1)Tp(33)

(4) magnetite(ss) + spinel(ss) + phase X + liquid at 1390° ± 10°C and Di(12)FATs(67)Tp(21)

These points are neither eutectic nor piercing points because of the nature of the seven-component system Fe-O-CaO-MgO-Al_2O_3-TiO_2-SiO_2 at the liquidus temperatures.

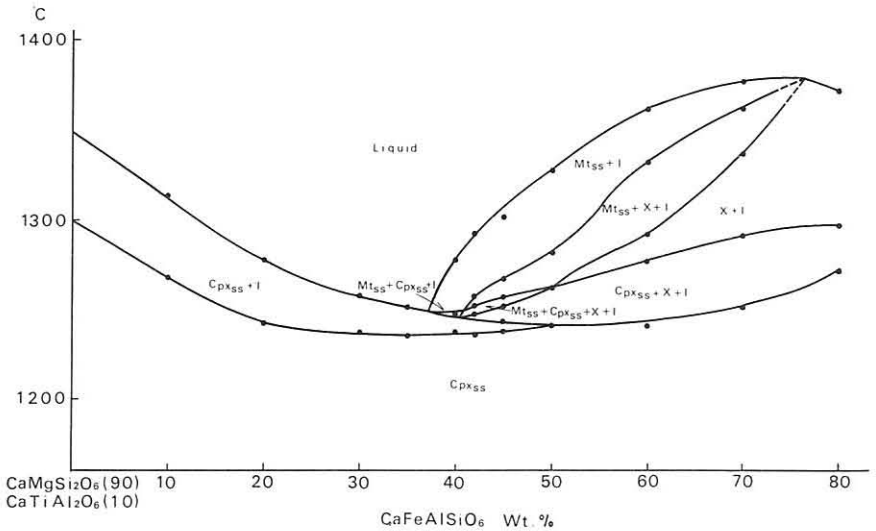

Fig. 2 Phase equilibrium diagram of 10% $CaTiAl_2O_6$ section.

* EPMA analyses revealed that this phase is hibonite.

Phase Relations at Subliquidus and Subsolidus

Clinopyroxene(ss), perovskite, forsterite, magnetite(ss), spinel(ss), melilite, anorthite, phase X, and hibonite are encountered as subliquidus and subsolidus phases throughout the area studied. Sections with 10, 20, and 30 wt.% Tp are shown in Figs. 2, 3, and 4 and a subsolidus diagram is given in Fig. 5.

Forsterite is consumed at the temperatures between 1253°C and 1228°C by the reaction with liquid. The compositions in the area rich in Di and FATs crystallize into clinopyroxene(ss) without any other phases as shown in Fig. 5. Maximum number of phase in a assemblage at solidus temperatures is six: clinopyroxene(ss) + perovskite + melilite + spinel(ss) + anorthite + liquid.

Since at higher temperature the reaction $Fe_2O_3 = 2FeO + \frac{1}{2}O_2$ takes place in air, the join is a part of the seven-component system. At lower temperatures, however, this reaction does not occur and the join can be treated as a six-component system Fe_2O_3-CaO-MgO-TiO_2-Al_2O_3-SiO_2.

10% Tp section is similar to the join Di-FATs (Hijikata and Onuma, 1969). A complete solid solution was found at subsolidus region. This clinopyroxene(ss) is stable until at least 900°C. The clinopyroxenes(ss) including more than 37% FATs melt incongruently to magnetite(ss) + liquid + gas between Di(53)FATs(37) and Di(50)FATs(40), to magnetite(ss) + phase X +

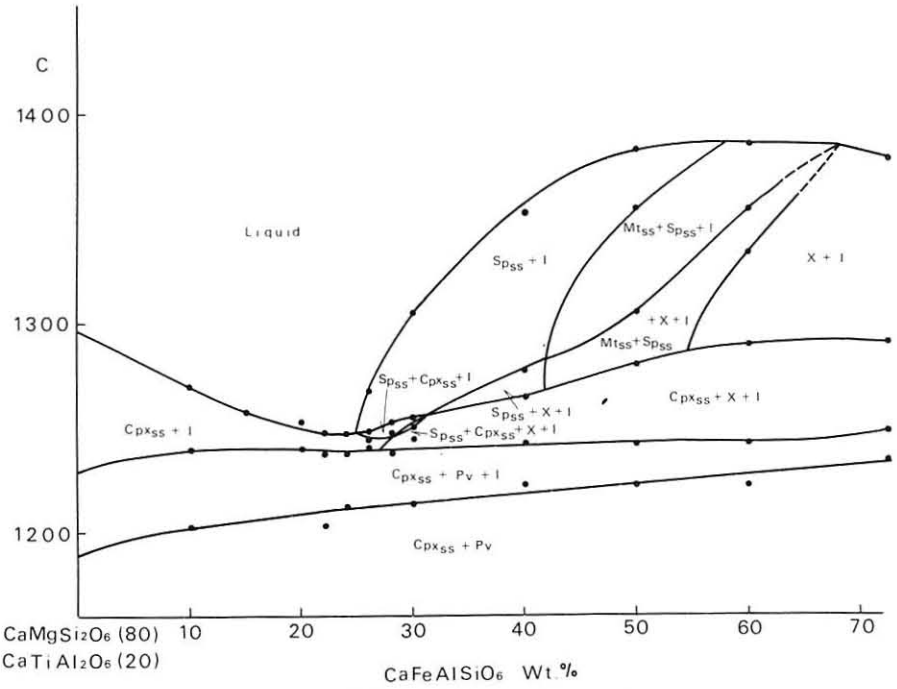

Fig. 3 Phase equilibrium diagram of 20% $CaTiAl_2O_6$ section. Abbreviations are the same as in Appendix.

liquid + gas between Di(50)FATs(40) and Di(42)FATs(48), and to phase X + liquid + gas between Di(42)FATs(48) and Di(10)FATs(80). The clinopyroxenes(ss) start to decompose above the temperatures at which reaction, $Fe_2O_3 = 2FeO + \frac{1}{2}O_2$, takes place.

In 20 wt.% Tp section, clinopyroxenes(ss) are no longer stable at subsolidus temperatures and decompose to clinopyroxene(ss) + perovskite. Spinel(ss) appears as a liquidus phase. This liquidus crosses the liquidus of clinopyroxene(ss) and the assemblage clinopyroxene(ss) + spinel(ss) + liquid appears.

In 30 wt.% Tp section, two assemblages are confirmed at subsolidus temperatures. One, the assemblage clinopyroxene(ss) + perovskite, is present between Di(70)FATs(0) and Di(39)FATs(31) and the other, the assemblage clinopyroxene(ss) + perovskite + melilite (+ anorthite), between Di(39)FATs(31) and Di(10)FATs(60).

40 wt.% Tp section is not shown. But at subsolidus temperatures at least three assemblages were confirmed; clinopyroxene(ss) + perovskite + melilite

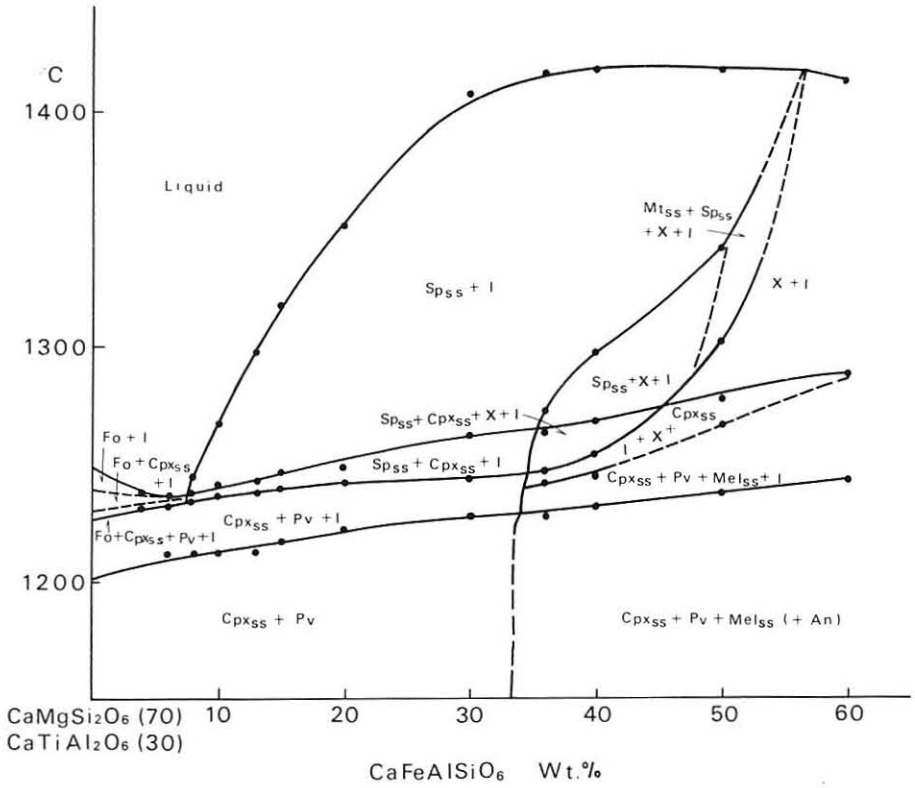

Fig. 4 Phase equilibrium diagram of 30% $CaTiAl_2O_6$ section. Abbrevations are the same as in Appendix.

+ spinel(ss) + anorthite, clinopyroxene(ss) + perovskite + spinel(ss) + anorthite and clinopyroxene(ss) + perovskite + anorthite + hibonite. Beside these, a field of clinopyroxene(ss) + perovskite + hibonite was assumed from the data of Onuma and Yagi (1971).

Possible Reactions at Subsolidus Temperatures

The phase assemblages at subsolidus temperatures are derived by the reactions between Di, FATs, and Tp. The following reactions are expected with increasing Tp.

(1) For the assemblage clinopyroxene(ss) + perovskite:

$$Di + Tp + FATs = \underset{\text{pyroxene(ss)}}{En + CaTs + FATs} + Pv$$

(2) For the assemblage clinopyroxene(ss) + melilite + anorthite + perovskite:

$$6Di + 3Tp + FATs = \underset{\text{pyroxene(ss)}}{5En + FATs} + 2An + Ak + Geh + 3Pv$$

(3) For the assemblage clinopyroxene(ss) + anorthite + spinel + melilite + perovskite:

$$7Di + 5Tp + FATs = \underset{\text{pyroxene(ss)}}{5En + FATs} + 3An + Ak + Geh + Sp + 5Pv$$

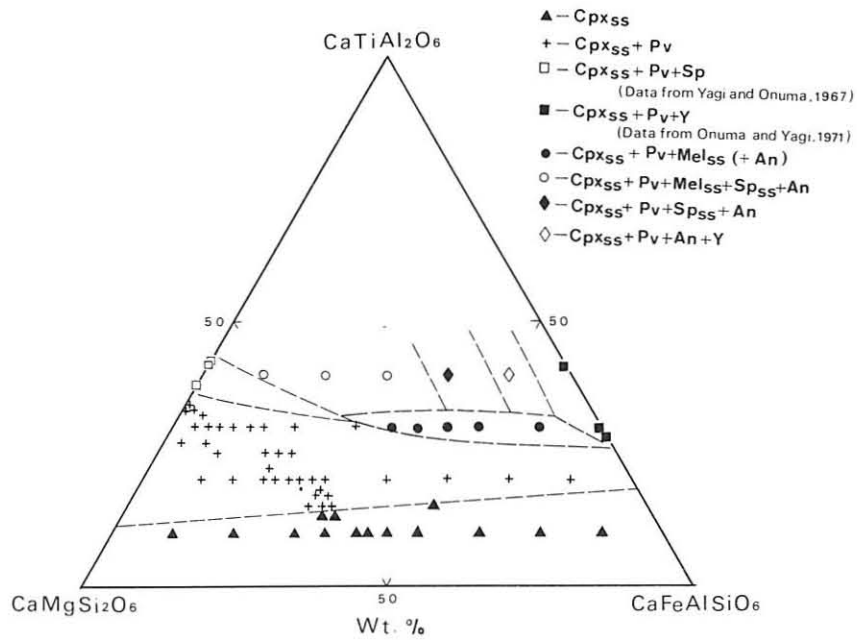

Fig. 5 Subsolidus diagram of the join $CaMgSi_2O_6$-$CaFe^{3+}AlSiO_6$-$CaTiAl_2O_6$. Abbreviations are the same as in Appendix.

Table 1 Unit-cell parameters of pyroxene solid solutions

Composition (wt.%) Di	FATs	Tp	a(Å)	b(Å)	c(Å)	β(°)	V(Å³)	Phase Assemblages
80	10	10	9.752(2)	8.899(2)	5.286(2)	106.03(3)	440.9(2)	Cpx
70	20	10	9.753(2)	8.877(2)	5.301(1)	106.01(3)	441.1(2)	Cpx
60	30	10	9.758(2)	8.870(2)	5.313(1)	106.04(2)	441.9(2)	Cpx
50	40	10	9.768(2)	8.860(1)	5.326(1)	106.04(2)	443.0(1)	Cpx
40	50	10	9.771(2)	8.843(2)	5.334(1)	106.01(2)	443.0(2)	Cpx
30	60	10	9.778(2)	8.830(2)	5.348(1)	105.95(2)	443.8(1)	Cpx
20	70	10	9.781(3)	8.811(2)	5.355(1)	105.90(3)	443.9(2)	Cpx
10	80	10	9.792(2)	8.796(2)	5.366(1)	105.82(2)	444.7(2)	Cpx
60	20	20	9.764(2)	8.860(2)	5.321(1)	106.07(2)	442.3(2)	Cpx + Pv
50	20	30	9.777(3)	8.838(2)	5.339(2)	106.07(3)	443.3(2)	Cpx + Pv
40	30	30	9.782(2)	8.823(1)	5.351(1)	105.99(2)	443.9(1)	Cpx + Pv
40	20	40	9.779(3)	8.826(2)	5.347(2)	106.07(3)	443.5(2)	Cpx + Pv + Mel + Sp + An
20	40	40	9.775(4)	8.788(3)	5.362(2)	106.02(4)	442.7(3)	Cpx + Pv + An + Sp

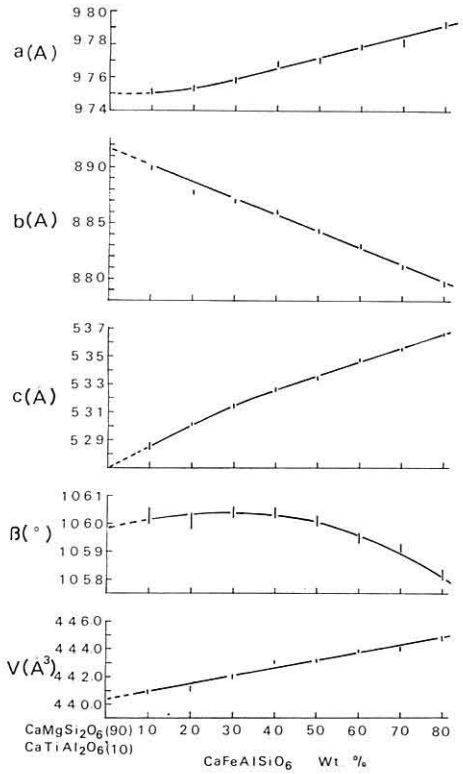

Fig. 6 The variation of unit-cell dimensions of the clinopyroxenes in 10% $CaTiAl_2O_6$ section.

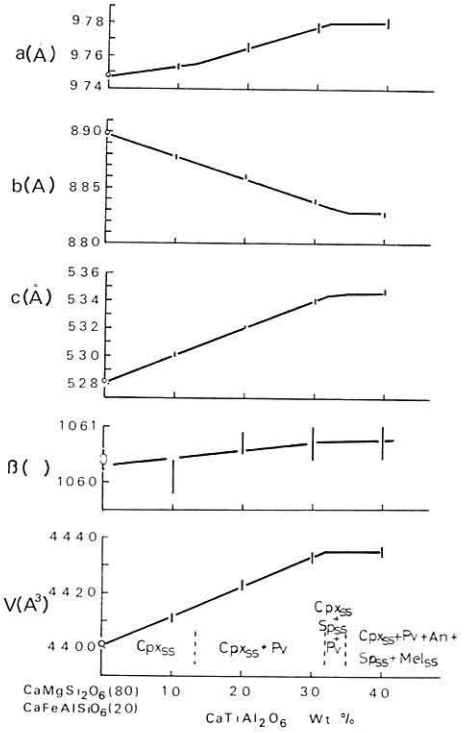

Fig. 7 The variation of unit-cell dimensions of the clinopyroxenes in the 20% $CaFe^{3+}AlSiO_6$ section.

(En = $MgSiO_3$, Ak = $Ca_2MgSi_2O_7$, Geh = $Ca_2Al_2SiO_7$, An = $CaAl_2Si_2O_8$)

It is noticed from the reactions mentioned above that clinopyroxene(ss) is expected to contain En and melilite could be a solid solution between Ak and Geh.

Nature of Clinopyroxene(ss) Obtained in the Join Di-FATs-Tp

Clinopyroxene forms prismatic crystals near liquidus but forms rounded grains in subsolidus region. They are always bright greenish yellow in color.

Unit-cell dimensions: Unit-cell dimensions of clinopyroxene(ss) crystallized at 1200°–1240°C for 24 hours-30 days are given in Table 1.

Table 2 Compositions of clinopyroxenes and coexisting glasses

No.	DFT-2		DFT-3		DFT-35		DFT-11	
Bulk comp. (wt.%)	Di 70 FATs 20 Tp 10		Di 60 FATs 30 Tp 10		Di 55 FATs 30 Tp 15		Di 50 FATs 30 Tp 20	
Run	1200°C, 84 hrs		1200°C, 84 hrs		1210°C, 30 days		1220°C, 23 hrs	
Phase Assemb.	cpx		cpx		cpx		cpx + pv	
	s.m.*	cpx	s.m.	cpx	s.m.	cpx	s.m.	cpx
SiO_2	43.71	43.33	40.59	41.09	37.82	37.96	45.04	35.20
TiO_2	3.36	3.32	3.36	3.41	5.04	4.98	6.72	5.76
Al_2O_3	8.41	8.51	10.48	10.50	12.62	12.70	14.76	15.00
Iron	6.47**	6.43**	9.70**	9.24**	9.70**	9.10**	9.70**	9.63**
MgO	13.03	12.67	11.17	10.63	10.24	9.73	9.31	9.10
CaO	25.02	25.46	24.71	25.69	24.59	26.05	24.47	24.55
Total		99.83		100.56		100.52		99.24
Si		1.62		1.54		1.44		1.35
Al^{IV}		0.37		0.46		0.56		0.65
Al^{VI}		0.00		0.00		0.01		0.03
Ti		0.10		0.10		0.14		0.17
Fe		0.18		0.26		0.26		0.28
Mg		0.71		0.60		0.55		0.52
Ca		1.02		1.03		1.06		1.01
O		6.00		6.00		6.00		6.00
Di		69.51		61.28		55.87		48.94
FATs		19.76		28.65		28.16		29.64
Tp		9.99		10.23		14.75		17.13
CaTs		0.22		0.43		1.53		3.27
En		0.00		0.00		0.00		0.00

* s.m. = Starting material

** Total iron as Fe_2O_3.

The unit-cell dimensions of the clinopyroxene(ss) crystallized in the 10% Tp join are plotted against FATs contents in Fig. 6. Dimensions of *a*, *c*, and *V* increase and *b* decreases linealy with increasing FATs, indicating the existence of a complete solid solution along this join. The variation patterns are very similar to those of clinopyroxenes(ss) in the join Di-FATs (Hijikata and Onuma, 1969).

Fig. 7 shows the variation of unit-cell dimensions of pyroxenes(ss) along the 20% FATs join. Dimensions of *a*, *c*, and *V* increase and *b* decreases with increasing Tp content up to 30% Tp throughout the fields of clinopyroxene(ss) single phase and clinopyroxene(ss) + perovskite. Beyond 30% Tp, the unit cell dimensions remain constant throughout the fields of clinopyroxene(ss) +

Table 2 (continued)

No.	DFT-9				DET-10			
Bulk comp. (wt.%)	Di 70 FATs 10 Tp 20				Di 60 FATs 20 Tp 20			
Run	1240°C, 72 hrs		1260°C, 14 hrs		1240°C, 72 hrs		1260°C, 14 hrs	
Phase Assemb.	cpx + pv		cpx + gl		cpx + pv		cpx + gl	
	s.m.	cpx	cpx	gl.	s.m.	cpx	cpx	gl.
SiO_2	41.28	42.12	45.81	40.18	38.16	38.45	38.59	37.34
TiO_2	6.72	5.62	3.74	7.14	6.72	5.97	5.05	7.30
Al_2O_3	10.64	10.35	7.47	10.98	12.70	12.38	13.02	13.73
Iron	3.23**	3.35**	2.81**	3.03**	6.47**	6.39**	6.54**	6.04**
MgO	13.03	13.02	14.20	11.89	11.17	11.23	11.23	10.63
CaO	25.11	25.26	25.75	26.63	24.79	25.24	25.18	25.89
Total		99.72	99.78	99.85		99.66	99.71	100.93
Si		1.57	1.69			1.45	1.46	
Al^{IV}		0.43	0.31			0.55	0.54	
Al^{VI}		0.03	0.01			0.00	0.04	
Ti		0.16	0.10			0.17	0.14	
Fe		0.09	0.08			0.18	0.19	
Mg		0.72	0.78			0.63	0.63	
Ca		1.01	1.02			1.02	1.02	
O		6.00	6.00			6.00	6.00	
Di		70.38				59.98		
FATs		10.37				19.76		
Tp		16.66				17.85		
CaTs		2.39				1.31		
En		0.00				0.30		

spinel(ss) + perovskite and clinopyroxene(ss) + perovskite + spinel(ss) + melilite + anorthite. This observation indicates that diopside structure can contains Tp molecule beyond the maximum amount (11%) proposed by Yagi and Onuma (1967).

Chemistry: Chemical compositions of the clinopyroxene(ss) crystallized at subliquidus and subsolidus temperatures are given in Table 2.

The clinopyroxenes(ss) in the single phase field of clinopyroxene(ss) have similar compositions to the starting materials, indicating that compositions in this field crystallize into clinopyroxene(ss) without any other phases.

It is observed that TiO_2 content in clinopyroxene(ss) increases even in the

Table 2 (continued)

No.	DFT-16		DFT-18	
Bulk comp. (wt.%)	Di 60 FATs 10 Tp 30		Di 40 FATs 30 Tp 30	
Run	1200°C, 48 hrs		1200°C, 48 hrs	
Phase Assemb.	cpx + pv		cpx + pv	
	s.m.	cpx	s.m.	cpx
SiO_2	35.73	36.52	29.49	29.57
TiO_2	10.07	9.37	10.07	9.20
Al_2O_3	14.92	14.82	19.05	18.78
Iron	3.23**	3.55**	9.69**	9.45**
MgO	11.17	11.85	7.44	7.15
CaO	24.88	25.15	24.24	25.48
Total		101.26		99.63
Si		1.35		1.15
Al^{IV}		0.65		0.85
Al^{VI}		0.00		0.01
Ti		0.26		0.27
Fe		0.10		0.27
Mg		0.65		0.41
Ca		1.00		1.06
O		6.00		6.00
Di		60.85		39.41
FATs		10.87		29.15
Tp		27.84		27.36
CaTs		1.31		2.18
En		1.31		0.00
Qz		−1.02		0.00

area of clinopyroxene(ss) + perovskite and the compositions of clinopyroxenes(ss) are similar to those of strating meterials. Perovskites are very small in amount in this area and therefore its appearance does not give too much difference in composition between clinopyroxene(ss) and starting materials. TiO_2 and Al_2O_3 content increases continuously with increasing Tp as suggested by the variation of the unit-cell dimensions and finally attains 9.20% TiO_2 and 18.57% Al_2O_3 as shown in Table 2.

Since the present experiments were performed in air, titanium and iron are in Ti^{4+} and Fe^{3+} state respectively. Therefore, the substitutions Mg + 2Si = Ti + 2Al(Ti:Al = 1:2) and Mg + Si = Fe^{3+} + Al(Fe^{3+}:Al = 1:1) are suggested. Fig. 8 support this substitution. The plotts of clinopyroxenes in the present join fall in the area between 1:1 line and 1:2 line. The slope for clinopyroxene(ss) in the section of constant Tp is parallel to 1:1 line and that of constant FATs to 1:2 line. Ti^{4+} does not enter into tetrahedral site (Dowty and Clark, 1973), but substitutes Mg. If the limit of TiO_2 in iron-free clinopyroxene is 3.7% (Yagi and Onuma, 1967) the present results imply that Fe^{3+} and Ti^{4+} coupling might be effective to form more Ti-rich clinopyroxene.

Recently Tracy et al. (1977) reported remarkable Ti-augite from Tahiti, which contains TiO_2 up to 8.73%. This is the most Ti-rich clinopyroxene ever

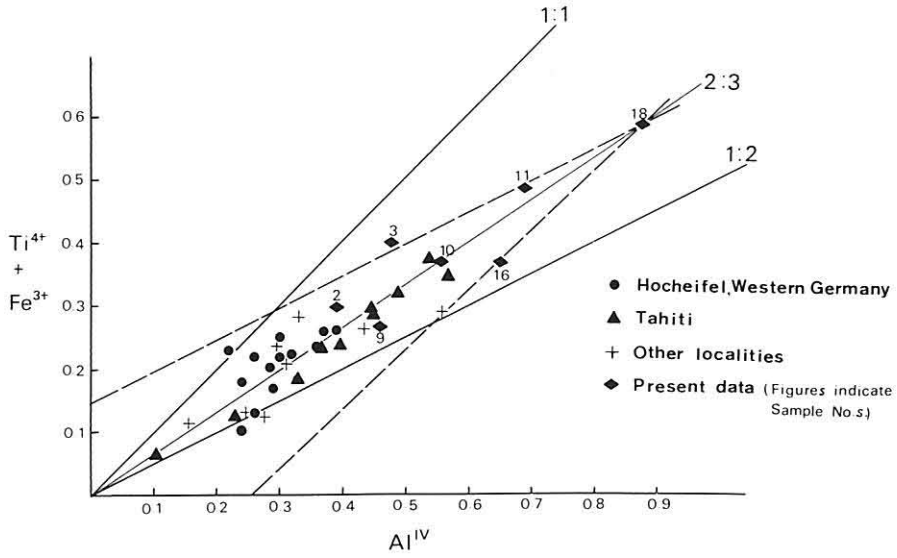

Fig. 8 Relation between Ti^{4+} + Fe^{3+} and Al^{IV} in Ti-rich clinopyroxenes from the various localities.
2: Di(70)FATs(20)Tp(10), 3: Di(60)FATs(30)Tp(10),
9: Di(70)FATs(10)Tp(20), 10: Di(60)FATs(20)Tp(20),
11: Di(50)FATs(30)Tp(20), 16: Di(60)FATs(10)Tp(30),
18: Di(40)FATs(30)Tp(30)

found in the earth. Ti-rich clinopyroxenes from various localities are plotted in Fig. 8. They fall in the area between 1:1 line and 1:2 line, implying the suggested substitution. Tahiti pyroxenes are plotted on 2:3 line, indicating the substitution $2Mg + 3Si = Ti^{4+} + Fe^{3+} + 3Al$.

Clinopyroxenes(ss) coexisting with liquid at 1260°C (from the composition Di(70)FATs(10)Tp(20)) contain less TiO_2 and Al_2O_3 than that crystallized at subsolidus temperature 1240°C. This indicates that clinopyroxene(ss) becomes richer in Ti and Al with proceeding of the crystallization. If the present join behaves as ternary system in Di-rich region, the liquid richer in Ti and Al than crystals is produced by the precipitation of clinopyroxene(ss) with falling temperature.

Other Crystalline Phases

Phase X and Hibonite: Phase X occurs as a prismatic crystal at liquidus and subliquidus temperatures, but sometimes forms rounded crystal when coexists with clinopyroxene. It shows distinct pleochriosm (X′, pale greenish yellow-brown; Z′, pale brown-dark reddish brown), weak birefringence, high relief, and straight extinction. Chemical composition of this phase is given in Table 3.

Table 3 Composition of phase X

SiO_2	12.10
TiO_2	1.73
Al_2O_3	22.18
FeO	42.12
MgO	7.52
CaO	15.30
	100.95
Cations per 24 oxygens	
Si	2.24
Ti	0.24
Al	4.86
Fe	6.58
Mg	2.10
Ca	3.06

Although molecular formular is still under the consideration, chemical analyses can be calculated in terms of $Fe^{2+}Fe^{3+}_2O_4$, $MgAl_2O_4$, and $Ca_3Si_2O_7$ (2:2:1), implying a Ca- and Si-bearing magnetite-spinel solid solution. However, the structure is no more isometric because of the presence of considerable amounts of Si and Ca in it.

Hibonite is a prismatic or hexagonal form. It shows high relief, pleochroism (X′, pale greenish brown; Z′, brown- reddish brown), and straight extinction. It is difficult to distinguish this phase from phase X under the microscope. However, it is easy to identify this phase with X-ray diffraction.

Other phases: Melilite occurs at lower temperature region together with other minute crystals and usually it was difficult to identify this mineral under the microscope. The strongest peak, 211, of melilite in X-ray diffraction ranges from 31.1° to 31.5° in 2θ, indicating that the melilite is assumed to be solid solution of akermanite, gehlenite and/or iron-gehlenite ($Ca_2Fe^{3+}AlSiO_7$).

Forsterite forms tabular crystal, showing high interference color.

Perovskite occurs usually in minute rounded or irregular form, slightly brown in color. Usually it can easily be identified by its high relief. Magnetite was found only at the liquidus and subliquidus temperatures in the FATs-rich region as octahedral form. As the color of magnetite varies from black to dark brown, it is expected that the magnetite is solid solution with spinel. Spinel shows octahedral form at liquidus and subliquidus temperatures, but is rounded grain at subsolidus temperatures. The color of spinel changes from pale green to dark green and becomes brown at lower temperatures in the FATs-rich region. Therefore, it is assumed that the spinel is a solid solution with magnetite.

Anorthite appears at subliquidus and subsolidus temperatures. In the present study it is rather difficult to identify this phase, because almost always anorthite is present as minute crystal together with other phases. In the X-ray diffraction, the strongest peak of anorthite, $\bar{2}04$, at 27.9° in $\bar{2}\theta$ is covered by a reflection of 220 of clinopyroxene. It is, therefore, also difficult to distinguish this mineral from clinopyroxene(ss) by X-ray diffraction pattern when a small amount of anorthite coexists with clinopyroxene(ss). In that case this phase is described with a blanket in Tables and Figures.

Implication To Natural Ti-rich Fassaitic Pyroxene

It is known that clinopyroxenes from alkalic rocks are higher in Ti and Al contents than those from tholeiitic rocks, and these ions are incorpolated in diopside as CaTs and Tp (Kushiro, 1960 and Yagi and Onuma, 1967). Onuma and Yagi (1971) and Huckenholz (1973) showed that the clinopyroxenes from such rocks as nephelinites, melilitites, and basanites contain not only CaTs and Tp, but considerable amount of FATs. Some authors reported clinopyroxenes from alkalic rocks containing more than 20% Tschermak's molecule (CaTs + FATs + FTs, $CaFe^{3+}_2SiO_6$, + Tp) (Sahama and Meyer, 1959; Tilley and Harwood, 1931, Huchenholz, 1973). Tracy et al. (1977) reported Ti-rich augite in alkali olivine basalt from Tahiti, which contains TiO_2 up to 8.7%.

Onuma and Yagi (1975) and Yoshikawa and Onuma (1975) suggested that at high f_{O_2} when enough Ca and Al are present Fe^{3+} enters into pyroxene as the form of FATs. Onuma and Yagi (1975) studied the join Di-CaTs-FATs and discussed its bearing on fassaitic pyroxene. However, the join studied by them does not includes Tp which is common in fassaitic pyroxenes from alkalic rocks. The join Di-FATs-Tp in the present study is therefore more reliable to the implication to natural fassaitic pyroxenes from alkalic rocks.

Schmincke and Duda (1977) showed that clinopyroxenes in basanite and nephelinite from Eifel, Germany have compositional zoning and Ti and Al of phenocrystic clinopyroxene increase from the core to the margin. Groundmass clinopyroxenes are always more richer in Ti than phenocrysts. Tracy et al. (1977) also pointed out the same phenomena.

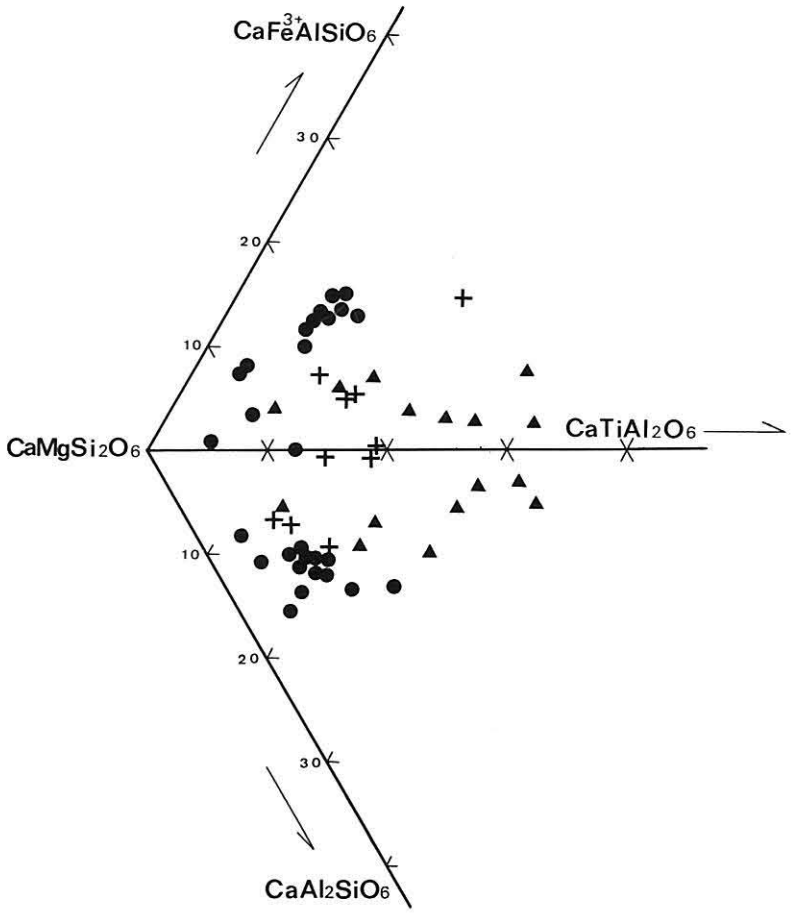

Fig. 9 Plots of natural Ti-bearing pyroxenes on the two balsal planes of Di-FATs-Tp and Di-CaTs-Tp. Symbols are the same as in Fig. 8.

These observations agree with the results of the present study and of the results by Onuma and Kimura (eleswhere in this volume). Natural Ti-bearing pyroxenes are plotted on the two basal planes of Di-FATs-Tp and Di-CaTs-Tp in Fig. 9. The Di-rich regions in these two joins behave as ternary system and, therefore, separation of clinopyroxenes(ss) at liquidus temperatures produces Ti-rich liquids and clinopyroxenes(ss) crystallized at later stage become richer in Ti, reflecting the composition of liquids from which they crystallized out. The trends of natural Ti-rich pyroxenes on the two joins are explained by the crystallization sequence mentioned here. Fig. 10 shows the trends of natural Ti-rich pyroxenes in the tetrahedron Di-CaTs-FATs-Tp. When Ti-rich pyroxenes are calculated in terms of pyroxene end- member, they involve usually these four molecules more than 80%. Therefore, it is reliable to use this quaternary system to trace the trends of Ti-rich pyroxenes. The trends are issued from Di towards Tp apex passing through the clinopyroxene(ss) field.

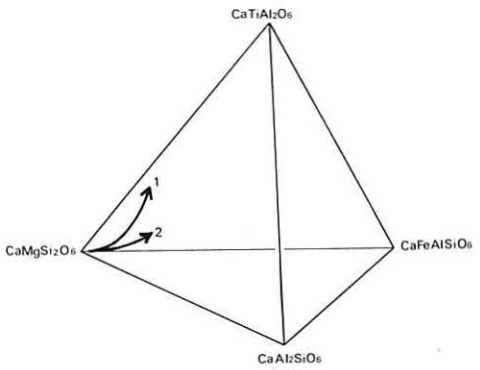

Fig. 10 The trend of natural Ti-rich pyroxene in the tetrahedron Di-CaTs-FATs-Tp.
1: Trend of Tahiti pyroxene, 2: trend of Hocheifel pyroxene.

Hollister and Gancarz (1971) and Dowty (1976) threw a question to the equilibrium crystallization of Ti-rich pyroxene because of occurrence of sector-zoning. Tracy et al. (1977) pointed out, however, that Tahiti Ti-rich pyroxene containing more than 7% TiO_2 does not have sector-zoning. The present experimental results indicate that the equilibrium crystallization of Ti-rich pyroxene is possible, and that if disequilibrium crystallization could occur to form Ti-rich pyroxene, it produces a residual liquid which has composition rich enough to crystallize more Ti-rich pyroxene.

Acknowledgement

This paper is dedicated to Prof. Kenzo Yagi on the occasion of his retirement from the chair. Under his guidance we became familiar with experimental methods of silicate system and were inspired to study experimen-

tal petrology. We wish to express our sincere gratitude for his guidance and encouragment during the study. We are grateful to the following persons: Mr. H. Kuwahata of the Faculty of Engineering, Hokkaido University for his help in E.P.M.A. analyses, Mr. S. Terada of our Department for his help in drawing figures, and Mrs. S. Yokoyama also of our Department for her typing the manuscript. Part of the cost for the present study was defrayed by the Grant for Scientific Research from the Ministry of Japan, No. 254268.

References

Dowty, E., 1976. Crystal structure and crystal growth: II. Sector zoning in minerals. *Am. Mineral.*, 61, 460-469.

Hijikata, K.and Onuma, K., 1969. Phase equilibria of the system $CaMgSi_2O_6$-$CaFe^{3+}AlSiO_6$ in air. *Jour. Japan. Assoc. Min. Pet. Econ. Geol.*, 62: 209-217.

Huckenholz, H.G., 1973. The origin of fassaitic augite in alkali basalt in suite of the Hocheifel area, Western Germany. *Contr. Mineral. Petrol.*, 40: 315-326.

Kushiro, I., 1960. Si-Al relation in pyroxenes from igenous rocks. Am. Jour. Sci., 258: 548-554.

Onuma, K. and Yagi, K., 1971. The join $CaFe^{3+}AlSiO_6$-$CaTiAl_2O_6$. *Abstract of Simp. Artf. Mineral.*

Onuma, K. and Yagi, K., 1971. The join $CaMgSi_2O_6$-$Ca_2MgSi_2O_6$-$CaTiAl_2O_6$ in the system CaO-MgO-Al_2O_3-TiO_2-SiO_2 and its bearing on the titanpyroxene. *Mineral. Mag.*, 38: 471-480.

Onuma, K. and Yagi, K., 1975. The join $CaMgSi_2O_6$-$CaAl_2SiO_6$-$CaFe^{3+}AlSiO_6$ in air and its bearing on fassaitic pyroxene. *Jour. Fac. Sci., Hokkaido Univ., Ser IV,* 16: 343-356.

Sahama, Th. G. and Meyer, A., 1958. *Exploration du Parc National Albert. 2,* Inst, Parcs Nat. Congo Belge, pp58.

Schmincke, H. and Duda, A., 1977. Quaternary parental and differentiated magmas from the Laacher See area (in press).

Tilley, C.E. and Harwood, H.F., 1931. The dolerite-chalk contact of Scawt Hill, Co. Antrim. The production of basic alkalic rocks by assimilation of limestone by basalt magma. *Mineral. Mag.*, 22: 439-468.

Tracy, J.R. and Robinson, P., 1977. Zoned titanian augite in alkali olivine basalt from Tahiti and the nature of titanium substitution in augite. *Am. Mineral.*, 62: 634-645.

Yagi, K. and Onuma, K., 1967. The join $CaMgSi_2O_6$-$CaTiAl_2O_6$ and its bearing on titanaugite. *Jour. Fac. Sci., Hokkaido Univ., Ser. IV,* 13: 463-483.

Yoshikawa, K and Onuma, K., 1975. The join $NaFeSi_2O_6$-$CaAl_2SiO_6$ at atmospheric and high pressure: I. Phase relation at 1 atm in air. *Jour. Japan. Assoc. Min. Pet. Econ. Geol.*, 70: 335-346.

(Received on Oct. 31, 1977)

Appendix Results of quenching experiments for the join $CaMgSi_2O_6$-$CaTiAl_2O_6$-$CaFe^{3+}AlSiO_6$ at 1 atm.

Composition(wt.%)			Temp.	Time	Results
Di	Tp	FATs	(°C)	(hrs.)	
80	10	10	1315	2	gl
			1300	2	cpx + gl
			1270	2	cpx + gl
			1265	2	fritted cake, cpx
70	20	10	1280	2	gl
			1270	2	cpx + gl
			1250	3	cpx + gl
			1245	3	fritted cake, cpx
60	30	10	1265	2	gl
			1260	2	cpx + gl
			1240	2	cpx + gl
			1235	3	fritted cake, cpx
55	35	10	1260	3	gl
			1255	12	cpx + gl
			1235	6	slightly glazed, cpx + gl
50	40	10	1280	2	gl
			1275	14	mt + gl
			1250	3	mt + gl
			1245	15	cpx + gl
			1240	2	cpx + gl
			1235	3	fritted cake, cpx
48	42	10	1295	12	gl
			1290	10	mt + gl
			1260	24	mt + gl
			1255	24	mt + x + gl
			1250	10	mt + x + cpx + gl
			1245	12	cpx + gl
			1230	24	slightly glazed, cpx
45	45	10	1300	2	mt + gl
			1270	4	mt + gl
			1260	3	mt + x + gl
			1255	12	cpx + x + gl
			1250	48	cpx + x + gl
			1245	48	cpx + gl
			1240	12	cpx + gl
			1235	6	fritted cake, cpx
40	50	10	1330	1½	gl
			1325	½	mt + gl
			1285	2	mt + gl
			1280	2	mt + x + gl
			1265	2	mt + x + gl
			1260	2	cpx + x + gl
			1245	15	cpx + x + gl
			1240	3	fritted cake, cpx

Appendix (continued)

Composition(wt.%)			Temp.	time	Results
Di	Tp	FATs	(°C)	(hrs.)	
30	60	10	1365	1½	mt + gl
			1335	½	mt + gl
			1330	1½	mt + x + gl
			1295	2	mt + x + gl
			1290	2	x + gl
			1280	2	x + gl
			1275	2	cpx + x + gl
			1245	15	cpx + x + gl
			1240	3	fritted cake, cpx
20	70	10	1380	1½	gl
			1375	½	mt + gl
			1365	½	mt + gl
			1360	1½	mt + x + gl
			1340	1½	mt + x + gl
			1335	½	x + gl
			1295	2	x + gl
			1290	2	cpx + x + gl
			1255	2	cpx + x + gl
			1250	2	fritted cake, cpx
10	80	10	1375	½	gl
			1370	1½	x + gl
			1300	2	x + gl
			1295	4	cpx + x + gl
			1275	13½	cpx + x + gl
			1270	2	fritted cake, cpx
54	33	13	1250	4	gl
			1245	5	cpx + gl
			1220	8	cpx + gl
			1215	6	fritted cake, cpx
52	35	13	1265	2	gl
			1260	6	mt + gl
			1255	10½	mt + gl
			1250	5	cpx + gl
			1215	6	cpx + gl?
			1210	720	fritted cake, cpx
55	30	15	1255	10½	gl
			1250	5	cpx + gl
			1230	5	cpx + gl
			1220	8	fritted cake, cpx + pv
53	32	15	1255	6	gl
			1250	4	mt + gl
			1245	5	mt + gl
			1240	12	mt + cpx + x + gl
			1235	4	cpx + gl
			1210	720	cpx + gl
			1200	12	fritted cake, cpx + pv

Appendix (continued)

Composition(wt.%)			Temp.	Time	Results
Di	Tp	FATs	(°C)	(hrs.)	
51	34	15	1270	11	gl
			1265	2	mt + gl
			1260	12	mt + sp? + x + gl
			1245	5	mt + sp? + x + gl
			1235	4	cpx + gl
			1230	6	fritted cake, cpx
53	30	17	1265	4	gl
			1260	3	sp + mt? + gl
			1255	4	sp + cpx + gl
			1250	5	cpx + sp + gl
			1220	8	cpx + gl
			1210	12	fritted cake, cpx + pv
51	32	17	1280	4	gl
			1275	2	mt + gl
			1265	4	mt + sp + gl
			1250	4	mt + sp + gl
			1245	3	mt + cpx + x + gl
			1240	6	cpx + gl
			1215	6	cpx + gl
			1210	720	fritted cake, cpx + pv
52	30	18	1275	2	gl
			1270	11	sp + gl
			1260	2	mt + sp + gl
			1250	4	mt + sp + gl
			1245	4	mt + sp + x + gl
			1240	4½	cpx + sp + x + gl
			1235	10	cpx + x + gl
			1230	6	cpx + gl
			1215	6	cpx + gl?
			1210	9½	fritted cake, cpx + pv
70	10	20	1270	8	gl
			1260	14	cpx + gl
			1245	4½	cpx + gl
			1240	15	cpx + pv + gl
			1215	20	cpx + pv + gl
			1200	72	fritted cake, cpx + pv
65	15	20	1260	2	gl
			1255	13	cpx + gl
60	20	20	1255	13	gl
			1250	24	cpx + gl
			1240	15	cpx + pv? + gl
			1205	18	cpx + pv + gl?
			1200	72	fritted cake, cpx + pv

Appendix (continued)

Composition(wt.%)			Temp.	Time	Results
Di	Tp	FATs	(°C)	(hrs.)	
58	22	20	1250	1½	gl
			1245	2	cpx + gl
			1240	2	cpx + gl
			1235	3	cpx + pv + gl
			1210	6	cpx + pv + gl
			1205	12	fritted cake, cpx + pv
56	24	20	1250	1½	gl
			1245	2	cpx + gl
			1240	2	cpx + gl
			1235	3	cpx + pv + gl
			1215	12	cpx + pv + gl
			1210	6	fritted cake, cpx + pv
54	26	20	1270	8	gl
			1265	5	sp + gl
			1250	14	sp + gl
			1247	6	sp + cpx + gl
			1245	18	cpx + gl
			1240	11½	cpx + pv + gl
50	30	20	1310	1	gl
			1300	1½	sp + gl
			1260	12	sp + gl
			1255	19	sp + cpx + gl
			1253	6	sp + cpx + x + gl
			1250	24	cpx + x + gl
			1245	4½	cpx + pv + gl
			1215	22	cpx + pv + gl?
			1210	23	fritted cake, cpx + pv
40	40	20	1355	1	gl
			1350	2	sp + gl
			1280	11	sp + gl
			1270	8	sp + mt + x + gl
			1260	3	x + cpx? + gl
			1245	24	x + cpx + gl
			1240	17	cpx + pv + gl
			1225	15	cpx + pv + gl
			1220	24	cpx + pv
30	50	20	1385	1	gl
			1380	1	sp + gl
			1360	9	sp + gl
			1350	2	sp + mt + gl
			1310	12	sp + mt + gl
			1300	2	sp + mt + x + gl
			1290	18	mt + x + gl
			1280	11	mt + x + gl
			1270	4	x + gl
			1245	24	cpx + x + gl
			1240	17	cpx + pv + gl
			1225	15	cpx + pv (+ gl)
			1220	24	fritted cake, cpx + pv

Appendix (continued)

Composition(wt.%)			Temp.	Time	Results
Di	Tp	FATs	(°C)	(hrs.)	
20	60	20	1390	1	gl
			1380	1	mt + gl
			1360	1½	mt + sp + gl
			1350	2	mt + sp + x + gl
			1340	11	mt + sp + x + gl
			1330	6½	x + gl
			1300	3	x + gl
			1290	18	cpx + x + gl
			1245	24	cpx + x + gl
			1240	17	cpx + pv + gl
			1225	15	cpx + pv (+ gl)
			1220	24	fritted cake, cpx + pv
10	70	20	1380	1	gl
			1375	1	x + gl
			1300	3	x + gl
			1250	14	cpx + x + gl
			1245	24	cpx + pv + gl
58	20	22	1245	12	gl
			1240	2	cpx + gl
			1235	3	cpx + gl
			1230	3	cpx + pv + gl
			1220	12	cpx + pv + gl
			1215	12	fritted cake, cpx + pv
65	10	25	1245	12	gl
			1240	2	cpx + gl
57	18	25	1270	4	gl
			1265	4	sp + gl
			1235	4	sp + gl
			1230	6	cpx + pv (+ gl)
			1210	9½	cpx + pv
55	20	25	1305	2	gl
			1300	12	sp + gl
53	22	25	1305	3	gl
			1300	12	sp + gl
70	3	27	1255	5	gl
			1250	12	fo + gl
			1245	20	fo + gl
			1240	12	fo + cpx + gl
66	7	23	1240	12	gl
			1235	3	cpx + gl
66	4	30	1240	36	gl
			1235	4	fo + cpx + gl
			1230	24	cpx + pv + gl

Appendix (continued)

Composition(wt.%)			Temp.	Time	Results
Di	Tp	FATs	(°C)	(hrs.)	
64	6	30	1240	36	gl
			1235	4	cpx + gl
			1230	24	cpx + pv + gl
			1215	24	cpx + pv + gl
			1210	12	fritted cake, cpx + pv
62	8	30	1250	1½	gl
			1245	2	sp + gl
			1240	2	sp + gl
			1235	3	cpx + pv + gl
			1215	12	cpx + pv (+ gl)
			1210	6	fritted cake, cpx + pv
60	10	30	1270	8	gl
			1265	5	sp + gl
			1245	12	sp + gl
			1240	12	sp + cpx + gl
			1230	17	cpx + pv + gl
			1215	12	cpx + pv + gl
			1210	15	fritted cake, cpx + pv
57	13	30	1300	1½	gl
			1295	2	sp + gl
			1245	3	sp + gl
			1240	2	cpx + pv + gl
			1215	12	cpx + pv + gl?
			1210	15	fritted cake, cpx + pv
55	15	30	1315	2	gl
			1310	1	sp + gl
			1245	3	sp + gl
			1240	2	cpx + pv + gl
			1220	18	cpx + pv + gl?
			1215	12	cpx + pv
50	20	30	1355	1	gl
			1350	2	sp + gl
			1250	14	sp + gl
			1245	12	cpx + sp + gl
			1240	12	cpx + pv + gl
			1225	18	cpx + pv + gl
			1220	18	fritted cake, cpx + pv
40	30	30	1410	1	gl
			1405	1	sp + gl
			1265	5	sp + gl
			1260	3	sp + cpx + gl
			1250	14	cpx + sp + gl
			1245	12	cpx + pv + gl
			1230	15	cpx + pv + gl
			1225	18	fritted cake, cpx + pv

Appendix (continued)

Composition(wt.%)			Temp.	Time	Results
Di	Tp	FATs	(°C)	(hrs.)	
34	36	30	1420	2	gl
			1415	2	sp + gl
30	40	30	1420	1	gl
			1415	1	sp + gl
			1295	2	sp + gl
			1290	14	sp + gl
			1255	12	sp + x + cpx + gl
			1250	6	cpx + x + pv + gl
			1240	12	cpx + x + pv + gl
			1235	17	cpx + mel + x + pv + gl
			1230	17	fritted cake, cpx + mel + pv (+ an)
20	50	30	1420	1	gl
			1415	1	sp + gl
			1345	2	sp + gl
			1340	14½	sp + x + gl
			1320	2	sp + mt + x + gl
			1300	2	x + gl
			1290	14	x + cpx? + gl
			1280	17	x + cpx + gl
			1260	6	x + cpx + mel + gl
			1240	12	cpx + x + mel + pv + gl
			1235	17	fritted cake, cpx + mel + pv (+ an)
10	60	30	1435	½	gl
			1430	½	x + gl
			1290	14	x + gl
			1280	5	x + cpx + pv? + gl
			1275	11½	x + cpx + mel + gl
			1260	6	x + cpx + mel + pv + gl
			1250	11	cpx + x + mel + pv + gl
			1240	12	fritted cake, cpx + mel + pv (+ an)
64	4	32	1250	1½	gl
			1245	2	sp + gl
			1240	2	sp + gl
			1235	3	sp + cpx + gl
			1230	3	sp + cpx + gl
			1220	12	cpx + pv + gl
			1215	12	cpx + pv + gl
			1210	6	cpx + pv
66	1	33	1240	12	gl
			1235	4	fo + gl
			1230	24	cpx + pv + gl?
			1215	24	cpx + pv + gl?
			1210	48	fritted cake, cpx + pv
65	2	33	1250	12	gl
			1245	5	sp + gl

Appendix (continued)

Composition(wt.%)			Temp.	Time	Results
Di	Tp	FATs	(°C)	(hrs.)	
50	10	40	1425	12	gl
			1420	2	sp + gl
			1320	13	sp + gl
			1315	12	sp + pv? + gl
			1235	12	sp + pv + gl
			1230	24	cpx + mel + pv + sp + an + gl
			1210	480	cpx + mel + pv + sp + an + gl
			1200	48	slightly fritted cake, cpx + mel + pv + sp + an
40	20	40	1445	½	gl
			1440	½	sp + gl
			1320	13	sp + gl
			1315	12	sp + pv + gl
			1240	5	cpx + mel + pv + sp + an + gl
			1210	480	cpx + mel + pv + sp + an + gl
			1200	48	fritted cake, cpx + mel + pv + sp + an
30	30	40	1460	2	sp + gl
			1340	15	sp + pv + gl
			1335	12	sp + pv + gl
			1260	24	sp + pv + gl
			1255	24	sp + pv + x + an? + gl
			1250	12	cpx + pv + mel + sp + an + gl
			1225	12	cpx + pv + mel + sp + an + gl
			1220	24	fritted cake, cpx + pv + sp + mel + an
20	40	40	1480	2	sp + gl
			1370	12	sp + gl
			1365	12	sp + h + gl
			1335	12	sp + h + gl
			1330	12	sp + h + pv + gl
			1300	12	sp + h + pv + gl
			1290	12	sp + x + h + pv + gl
			1260	24	sp + x + h + pv + gl
			1255	12	cpx + x + an + sp + pv + gl
			1235	12	cpx + x + an + sp + pv + gl
			1230	24	fritted cake, cpx + pv + an + sp
10	50	40	1455	½	h + gl
			1395	½	h + gl
			1390	½	h + sp + gl
			1320	9	h + sp + gl
			1315	12	h + sp + pv + gl
			1280	20	h + sp + pv + gl
			1270	12	cpx + h + mel + pv + gl
			1240	5	cpx + h + pv + gl
			1235	12	fritted cake, cpx + h + pv + an

cpx,clinopyroxene; pv,perovskite; mt,magnetite; x,phase X;
sp,spinel; fo,forsterite; mel,melilite; an,anorthite; h, hibonite; gl,glass